ACSNANO
www.acsnano.org
ARTICLE

Flexibly and Repeatedly Modulating Lasing Wavelengths in a Single Core–Shell Semiconductor Microrod

Hua Zong,[†] Yue Yang,[†] Chuang Ma,[§] Xiaohui Feng,[†] Tiantian Wei,[†] Wei Yang,[†] Junchao Li,[†] Junze Li,[‡] Liping You,[†] Jian Zhang,[‡] Mo Li,[‡] Caofeng Pan,*[,§] Xiaodong Hu,*[,†] and Bo Shen[†]

[†]State Key Laboratory of Artificial Microstructure and Mesoscopic Physics, School of Physics, Peking University, Beijing 100871, P. R. China

[§]Beijing Institute of Nanoenergy and Nanosystems, Chinese Academy of Sciences; National Center for Nanoscience and Technology (NCNST), Beijing 100083, P. R. China

[‡]Microsystem and Terahertz Research Center, China Academy of Engineering Physics, Chengdu 610200, Sichuan, P. R. China

Supporting Information

ABSTRACT: **Modulating lasing wavelength flexibly and repeatedly on a single rod is essential to the practical applications of micro/nanorod lasers. In this paper, a structure that decouples the gain medium and optical cavity is proposed, where the corresponding mechanism for the lasing wavelength shift is explained. Based on the above structure, one kind of wavelength continuously variable lasers is achieved on a single GaN/InGaN core–shell microrod without modifying the geometry of the resonant cavity or cutting the microrod. By using this method, lasing wavelength can be modulated from 372 to 408 nm flexibly and repeatedly in a 10 μm facilely synthesized microrod. This approach demonstrates a big application potential in numerous fields consisting of optical telecommunication and environmental monitoring.**

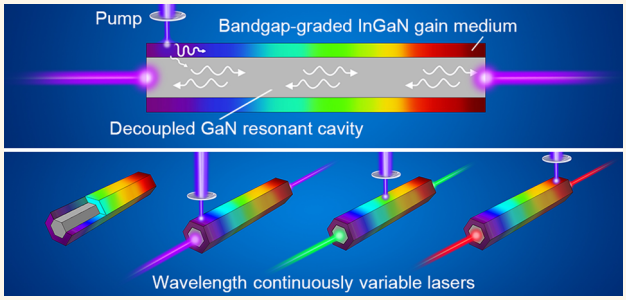

KEYWORDS: *single micro/nanorod laser, wavelength continuously variable, decoupling, core–shell, gallium nitride*

Semiconductor micro/nanorod lasers, with compact size, strong optical confinement, and sufficient optical gain,[1] have recently attracted considerable interest, since they are desirable modules for integrated photonic applications. Furthermore, for certain fields, such as saturated spectroscopy,[2] environmental monitoring,[3] and optical communication,[4] the wavelength continuously variable lasers (WCVLs) are specifically required.

According to the dependence of the output wavelength on the bandgap of the material, stimulating multiple nanorods with a different bandgap is an understandable method to achieve different lasing wavelengths.[5−9] However, this method is limited by the fact that the obtained lasing wavelengths are discrete and the preparation process is complicated. From a practical point of view, it is necessary to achieve WCVL on a single rod.

In order to modulate the lasing wavelength on a single rod, it is natural to synthesize a bandgap-graded rod, for which the rod usually serves as both gain medium and resonant cavity. In this case, when the narrow bandgap end of the rod is locally excited by a focused pulse laser, interband optical absorption cannot take place, and light power easily reaches the threshold and starts lasing.[10,11] In comparison, when the wide bandgap end is excited, light power will transmit along the bandgap-decreasing direction through incessantly repeated band-to-band reabsorption and re-emitting processes. In this case, no lasing is observed even when we increase the pump intensity.[12] Based on the above situation, despite moving the laser excited spot, the above asymmetric bandgap absorption frames the lasing wavelength in the PL range of the narrow-bandgap end. Hence, if a WCVL realized by a single bandgap-graded rod is desired, it is necessary to cut off the narrow-bandgap end section by section.[13] Instead of cutting, multicolor lasing also can be realized on a single bandgap-graded CdSSe nanoribbon by a multiscattering effect at morphology defect sites of the nanoribbon. However, the lasing wavelength is difficult to control and modulate because of the random distribution of defects.[14]

Received: February 28, 2017
Accepted: May 28, 2017
Published: May 28, 2017

ACS Publications © XXXX American Chemical Society

DOI: 10.1021/acsnano.7b01417
ACS Nano XXXX, XXX, XXX–XXX

Besides, other physical mechanisms such as the absorption−emission−absorption process and Burstein−Moss effect also have been utilized to tailor wavelength on a single nanorod with fixed composition.[15−17] This method is limited by the inevitable narrow photoluminescence (PL) range and the gain profile of the nanorod. Another idea is to modify the geometry of resonant cavity depending on the resonant F−P cavity theory. As for this method, the wavelength shift is confined within 10 nm.[18,19] As is known to all, for commercial application, it is essential for the WCVL to be synthesized facilely and modulated in a wide wavelength range flexibly and repeatedly. Therefore, further investigation is required to meet these demands by another approach.

In this work, we propose a core−shell structure to obtain high-performance and low-cost WCVL by decoupling a gain medium and resonant cavity. In our core−shell structure, the bandgap-graded InGaN shell provides the gain medium, while the high-quality GaN core acts as the shared resonant cavity. When excited by an external ultraviolet laser spot, energy can be absorbed strongly and locally by the excited position with a certain indium composition. Then the emission with the corresponding wavelength can oscillate in the shared GaN core without mutual absorption. Therefore, a tunable laser can be obtained by simply changing the excited position without additional operation. In this way, we fabricate a WCVL with a length of 10 μm and a wavelength variation from 372 to 408 nm (variation rate of 3.6 nm/μm). With the facile fabrication process and the large variation range, our WCVL method demonstrates a big application potential in numerous fields.

RESULTS AND DISCUSSION

Schematic diagram of the structure that decouples the gain medium and resonant cavity has been drawn in Figure 1. In general, main body of the structure is a GaN core, which is evenly wrapped by the bandgap-graded InGaN shell layer. When excited by an external ultraviolet laser spot, external laser photo energy can be absorbed strongly and locally by the excited position of InGaN shell. When the thickness of shell layer is more than dozens of nanometers, the GaN core can hardly be excited by the external laser at room temperature (see Figure S1 of the Supporting Information).[20,21] Since the shell has a quite small thickness, it is difficult for the InGaN shell to confine the light and support optical resonant modes. So most of the emission from the InGaN gain medium is coupled into the GaN core which acts as an optical microcavity and generates resonant modes.[22−24] When the narrow bandgap end of the InGaN shell layer is locally excited, whether the residual light in the shell layer or the main part of light coupled into the core, in the transmission of positive direction, interband optical absorption cannot take place, and the light easily reaches the threshold and starts lasing. For the other case, when the wide bandgap end of the InGaN shell layer is locally excited with the same power, the situation is different. The residual light in the shell layer will transmit along the negative direction through incessantly repeated band-to-band reabsorption and re-emitting processes. The wavelength of the light will change and redshift continuously, so that the residual light in the shell layer can hardly be amplified by stimulated emission. The main light coupled into the core will transmit unimpededly along the negative direction without strong absorption and generate resonant modes, finally lasing, as shown in Figure 1a. Hence, the lasing wavelength will correspond to the indium composition of the laser excited position, which is completely different from the case of the bandgap-graded rod. We can realize the emission and gain of different wavelengths by changing the indium composition of the shell layer along the growth direction of single rod. Then the emission with the corresponding wavelength can oscillate in the shared GaN core without mutual absorption.

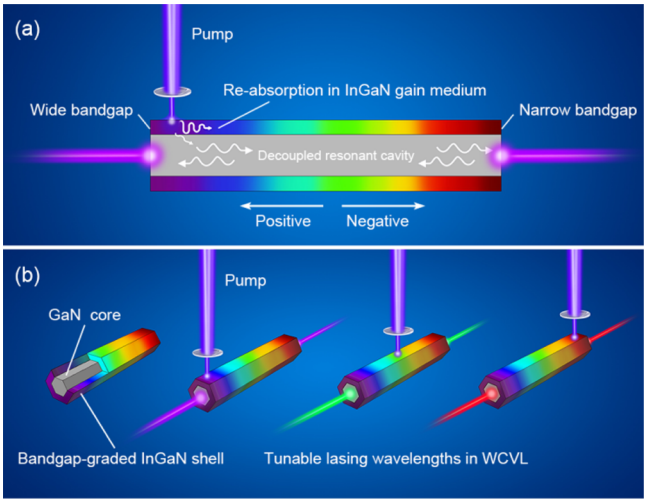

Figure 1. (a) Schematic diagram of the structure that decouples the gain medium and resonant cavity. (b) Effect diagram of WCVLs, which can be obtained by simply changing the excited position without additional operation.

After the size parameters of core−shell structure are elaborately designed and optimized, the vast majority of optical field intensity will be distributed in the GaN core. This means that the gain medium and resonant cavity can sufficiently decouple, and the tunable laser can be obtained by simply changing the excited position without additional operation, as shown in Figure 1b. In order to realize this, the GaN core is supposed to be obtained with a high-quality waveguide and resonant cavity. The InGaN shell should be deposited uniformly, where the bandgap variation is expected to be considerably large.

To clarify the nature of decoupling, we performed a two-dimensional (2D) finite-difference eigenmode simulation to determine the optical field distributions of the modes supported by the micro/nanorod laser and optimize the size parameters of the core−shell structure. In the simulation, the operation wavelength is set to be 390 nm, where the corresponding indium composition in InGaN is 8%, where the refractive indexes of the InGaN shell layer and GaN core are 2.671 and 2.69,[25] respectively. We fix the thickness of the InGaN shell layer to be 50 nm and change the radius of the regular hexagon GaN core ranging from 50 nm to 1 μm. It can be seen from Figure 2a that as the radius of the GaN core increases, more and more fundamental mode optical field intensity is distributed in the core. When the radius of the core reaches 1 μm, the vast majority of fundamental mode optical field intensity (99.9%) is distributed in the GaN core and the proportion tends to be saturated. The inset of Figure 2b shows the 2D optical field distribution of the fundamental mode supported by the core−shell structure (with core radii of 75 nm and 1 μm), which is consistent with the above conclusions. The higher-order modes contribute significantly to the laser performance, as they usually exhibit higher reflectivities and

DOI: 10.1021/acsnano.7b01417
ACS Nano XXXX, XXX, XXX−XXX

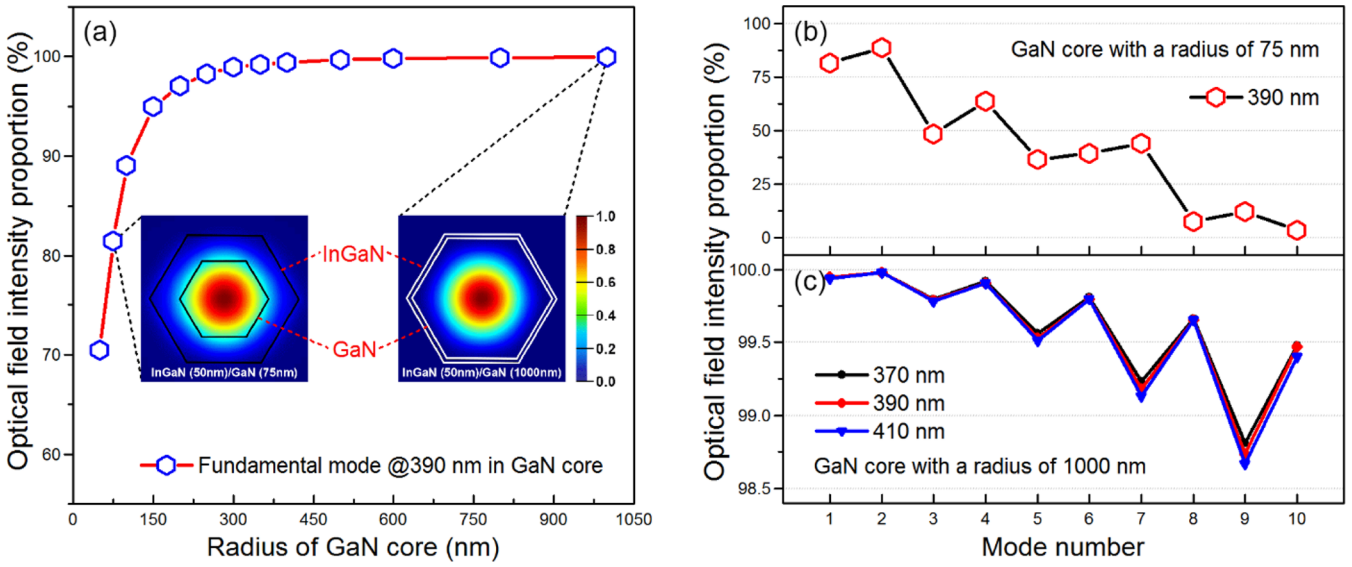

Figure 2. (a) Under different size parameters of core−shell structures, the proportion of the optical field intensity in the core to the total optical field intensity. Inset: 2D optical field distribution of the fundamental mode supported by different core−shell structures. (b) Setting the radius of GaN core to be 75 nm and the operation wavelength to be 390 nm, the proportion of the core optical field intensity to the total optical field intensity of different modes. (c) Setting the radius of GaN core to be 1 μm and changing the operation wavelength from 370 to 410 nm, the proportion of the core optical field intensity to the total optical field intensity of different modes.

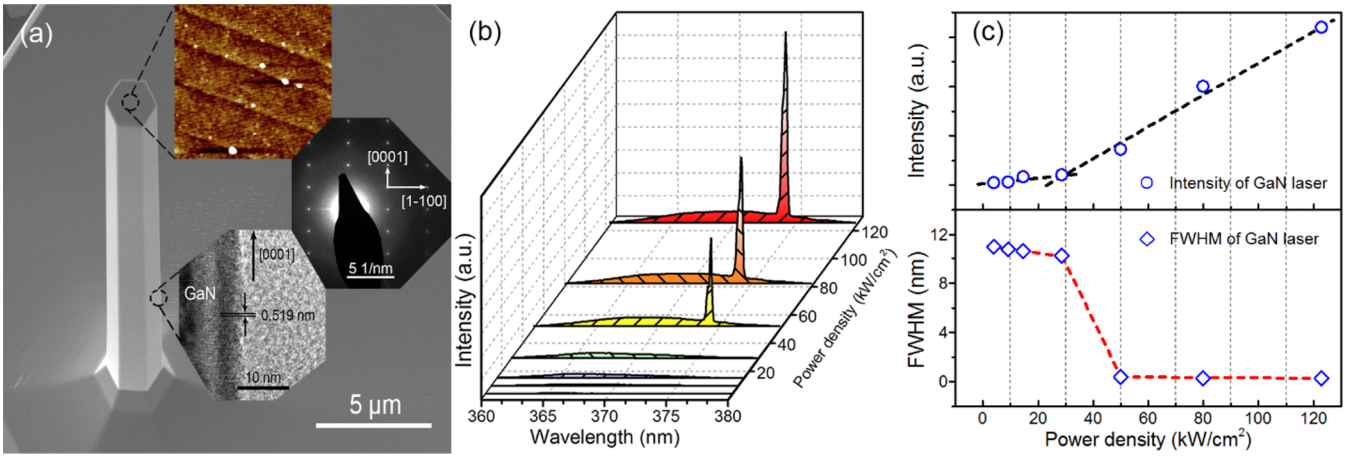

Figure 3. (a) SEM image of the GaN microrod structure with uniform side wall and regular hexagonal cross sections. Inset: AFM image of the top surface with a RMS of 0.147 nm. A selected-area diffraction pattern recorded along the $[11\bar{2}0]$ zone axis shows that GaN core grows along [0001] direction. High-resolution TEM image of a typical microrod. (b) Spectrum of optically excited lasing in a 10 μm long GaN microrod. (c) Threshold curve and fwhm of spectrum for the same lasing microrod.

thus lower thresholds than the fundamental mode.[26−29] We also performed 2D finite-difference eigenmode simulation on nine higher-order modes for the GaN cores with different radius values. For the core−shell nanorod with a core radius of 75 nm, most of the optical field leaks into the InGaN shell layer as the mode number increases. For the core−shell microrod with a core radius of 1 μm, though the higher-order modes reveal intensity profiles that are shifted toward the side facets of the microrod, the vast majority of optical field intensity is still distributed in the GaN core (see Figure S2 of the Supporting Information). In order to characterize the optical field distributed in the GaN core more exactly, we calculate the proportion of the optical field intensity in the core to the total optical field intensity. From Figure 2b, we find that for the core−shell nanorod with a core radius of 75 nm, the proportion decrease from 88.6% to 3.5% as the mode number increases.[22,23] However, for the core−shell microrod with a core radius of 1 μm, the proportion is 98.74% at least, as shown in Figure 2c red line. Thus, for the operation wavelength of 390 nm, the gain medium and the resonant cavity are decoupled sufficiently when the InGaN shell layer is 50 nm and the radius of GaN core reaches 1 μm. We also simulate other operation wavelengths, such as 370 and 410 nm, whereas the corresponding indium composition in InGaN is 2% and 14%, where the refractive indexes of InGaN are 2.732 and 2.57, respectively.[25] The refractive indexes of GaN at 370 and 410 nm are 2.737 and 2.585,[25] respectively. We fix the radius of the GaN core to be 1 μm and the thickness of the InGaN shell to be 50 nm. As shown in Figure 2c, black and blue lines, even though the operation wavelength changes from 370 to 410 nm, the proportion of the optical field intensity in the core is at least 98.67% of the total optical field intensity. Based on the above

DOI: 10.1021/acsnano.7b01417
ACS Nano XXXX, XXX, XXX−XXX

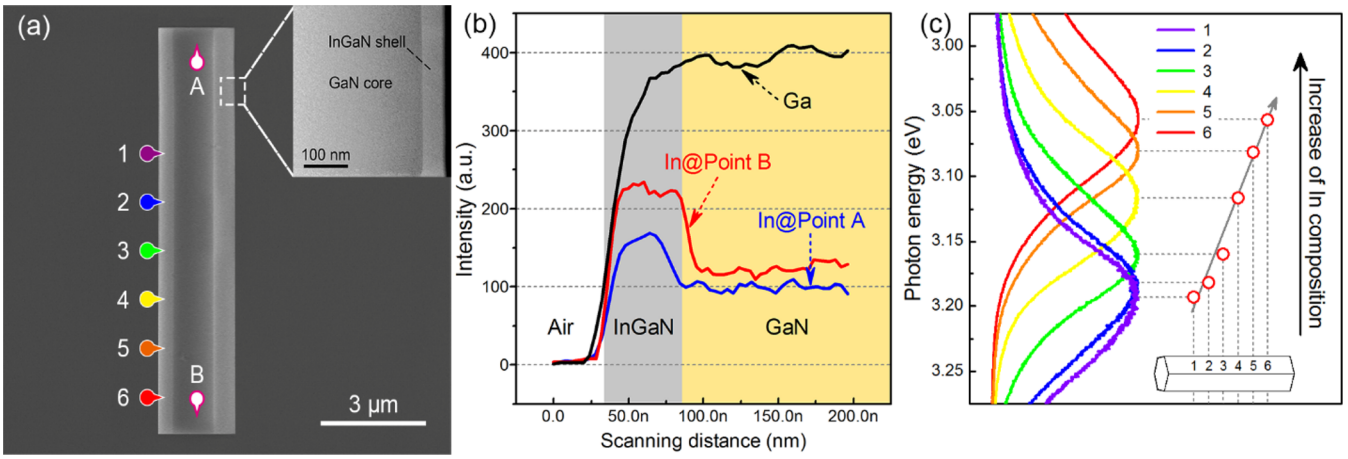

Figure 4. (a) Core−shell structure transferred to a sapphire substrate. Inset: STEM HAADF image of core−shell structure. (b) Line scan STEM HAADF energy spectrum is measured at positions A and B perpendicular to the growth direction. (c) Microphotoluminescence spectrum image of different positions on the same GaN/InGaN core−shell rod locally excited by a 325 nm continuous wave laser.

results, a good decoupling effect in the core−shell structure can be formed when the radius of the GaN core reaches 1 μm, even though the indium composition of InGaN shell layer varies from 2% to 14%.

The GaN core is the waveguide layer of GaN/InGaN core−shell WCVL, so the synthesis of a high-quality waveguide and resonant cavity is one of the prerequisites to achieve a WCVL. More importantly, the quality of GaN core directly determines the growth of InGaN shell layer. After the size parameters of core−shell structure is elaborately designed and optimized, the performance of the GaN core is of great concern and will be grown and investigated first, prior to examining the properties of the GaN/InGaN core−shell rods. Figure 3a shows the scanning electron microscopy (SEM) image of the GaN core structure with a regular hexagonal cross section. Through our statistics, radii of most GaN microrods are between 1 and 1.5 μm, which satisfy the size parameter for decoupling. The smooth surface morphology is very important for waveguiding without significant loss from surface emission and can make the InGaN shell grow rather easily and uniformly on the surface of GaN core. From the atomic force microscope (AFM) image shown in the inset of Figure 3a, we can clearly see the single layer atomic step and the root-mean-square (RMS) roughness of the top surface is 0.147 nm. It demonstrates that the microrod has a sharp facet, which is very important to form a high-quality resonant cavity. A selected-area diffraction pattern recorded along the $[11\bar{2}0]$ zone axis shows that GaN core grows along [0001] direction. A high-resolution transmission electron microscopy (TEM) image of a typical microrod reveals a high-quality single-crystal wurtzite structure, and the lattice constant along the *c*-axis is obtained as c = 5.19 Å, as shown in the inset of Figure 3a.

To evaluate the quality of the waveguide and the resonant cavity more carefully, the threshold characteristics of the GaN microrod laser were measured and analyzed. The threshold condition for laser oscillation is that the round-trip gain inside the microrod must equal the round-trip losses:[15,30]

$$\Gamma_0 g_{\mathrm{th}}^0 = \alpha_{\mathrm{w}} + \alpha_{\mathrm{m}} \quad (1)$$

where Γ_0 is the confinement factor, g_{th}^0 is the threshold gain (the threshold pump intensity is proportional to g_{th}^0), α_{w} is the waveguide loss, and α_{m} accounts for the loss at the interface (the mirror loss). Figure 3b,c shows the results of optically excited lasing in a 10 μm-long GaN microrod. Above the threshold power density of 30 kw/cm^2, a narrow peak with a fwhm of 0.3 nm is developed at 374 nm (3.32 eV). We can observe the simultaneous line narrowing and superlinear increase of intensity at pump densities as low as 30 kw/cm^2, to our knowledge, a very low threshold room-temperature lasing reported for GaN materials.[30,31] When Γ_0 keeps constant, g_{th}^0 is lower and α_{w} and α_{m} are smaller. This means that the GaN core we synthesize forms a high-quality waveguide and resonant cavity, which provides a prerequisite for the realization of a core−shell WCVL.

The synthesis of a uniform bandgap-graded InGaN shell with considerably large bandgap variation is the other prerequisite to achieve a core−shell WCVL. Hence, physical and optical properties of the bandgap-graded InGaN shell have been investigated. To precisely evaluate the thickness and the variation of indium incorporation of the InGaN shell rod along the growth direction, scanning transmission electron microscopy high-angle annular dark field (STEM HAADF) images are taken along the rod, as shown in the inset of Figure 4a. The thickness of the shell is about 50 nm uniformly distributed along the growth direction of [0001]. The distribution of indium along the growth direction is investigated using a STEM HAADF energy spectrum.[32] In Figure 4b, line scan energy spectrum is measured at positions A and B perpendicular to the growth direction and from which we can find obviously different indium compositions between them. Figure 4c presents the microphotoluminescence spectra of the same GaN/InGaN core−shell rod local excited by a continue wave laser (325 nm). The emitting peak photon energy of the shell gradually changes from 3.2 eV at position 1 (388 nm) to 3.05 eV at position 6 (406 nm). The possible explanation is the higher rate of indium incorporation into the InGaN shell in the upper part of the rod (position B) than in the lower part of the rod (position A). This may be due to the longer surface migration length of the indium adatom compared to the gallium adatom and the lower dissociation rate of indium caused by the slightly lower surface temperature on the upper part *versus* the lower part.[33,34] These two effects can contribute to the indium incorporation gradient of the InGaN shell layer along the growth direction. Through the above experimental verification, we have obtained micron radius sized GaN cores

DOI: 10.1021/acsnano.7b01417
ACS Nano XXXX, XXX, XXX−XXX

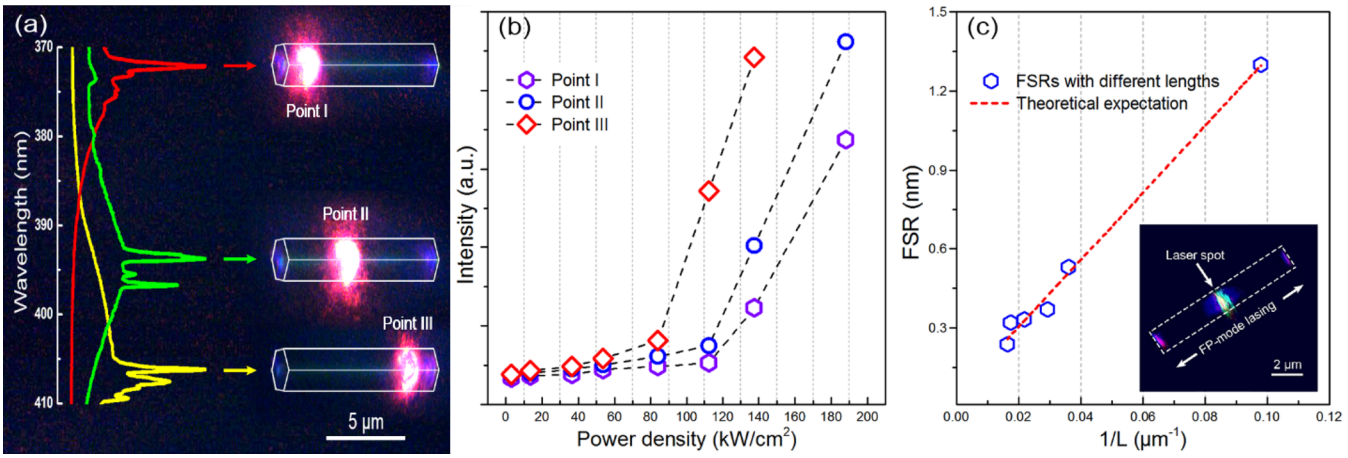

Figure 5. (a) Lasing spectrum and real-color optical microscope image of different excited points. (b) The power dependence of different excitation points (different lasing wavelengths). (c) The influence of GaN cores length on FSR and the theoretical value for FP-type resonances. Inset: real-color optical microscope image of a GaN core excited by a Nd:YAG laser (355 nm) under high excitation power densities (above the threshold).

uniformly wrapped by a large bandgap variation InGaN shell structure.

In the experiments on laser excitation for WCVL, as shown in Figure 5a, the excited point changes from point I to point III, and we collect the complete emission from the microrod rather than one end face of that. We can get different lasing wavelengths at different points, and the lasing wavelength can be changed from 372 to 408 nm in this 10 μm facilely synthesized rod. The variation rate (lasing wavelength variation divided by the length of the rod) is as high as 3.6 nm/μm, which is rarely reported.[13−15] The power dependence of the different excited points is shown in Figure 5b. From this figure we can see that the excitation thresholds of different excitation points are concentrated near 100 kw/cm^2. The threshold of point I (372 nm) is higher than that of point III (408 nm).[14,27]

In order to give a qualitative analysis, we must determine the lasing oscillation mode of that core−shell WCVL that we get first. In our core−shell structure, a vast majority of the optical field intensity is distributed in the GaN core for transmission and resonance, which has been proved in Figure 2. So the lasing oscillation mode of core−shell structure will be determined by the lasing oscillation mode of the GaN core. In order to clarify the lasing oscillation mode of the GaN core, we study the influence of GaN microrods length on free spectral range (FSR). Sonication process is used to remove microrods from the growth substrate in an alcoholic solution and transfer to a sapphire substrate. A Nd:YAG laser (355 nm) is used as the excitation source. For Fabry−Perot (FP)-type resonances, the relationship follows the equation:[35]

$$\mathrm{FSR} = \lambda^2/2n(\lambda)L \tag{2}$$

$n(\lambda)$ is the effective group refractive index at lasing wavelength λ. In our lasing wavelength range, $\lambda^2/2n(\lambda)$ is about 1.4×10^4 nm^2, and the relationship between FSR and L^{-1} has been drawn as red line in Figure 5c. For our GaN microrods, the relationship between FSR and L^{-1} is well consistent with theoretical expectations. So for most of the GaN microrods with radii of 1−1.5 μm, FP-type resonances have been proved during the lasing process. At low excitation power densities, spontaneous emission is observed from both the body and ends of the microrod. When increasing the excitation power intensity, the emission from the ends increases and becomes dominant, as shown in the inset of Figure 5c, indicating strong FP cavity properties and eventually forming a laser. This is consistent with the lasing image observed in Figure 5a. The above experimental results indicate that FP-type modes are dominant in the mode competition with whispering gallery modes (WGMs) for the GaN core. This may be due to two reasons: One is the two smooth end faces of the microrod can form a high-quality FP cavity, and the other one is that the radii of the samples used in our experiments are almost 1 μm, and it does not have enough advantage to enable low-loss WGM cavities.[36,37] So it is easier to observe the FP-type lasing, which means that the lasing modes for our core−shell WCVL are FP-type modes.

After determining the lasing oscillation mode of our core−shell WCVL, we try to qualitatively analyze the threshold of different excitation points (different lasing wavelengths). In our core−shell WCVL structure, optical field leakages into the InGaN shell layer are very little (as shown in Figure 2), so the waveguide loss for InGaN shell can be ignored. Under a FP-type mode, the threshold condition of core−shell WCVL is illustrated in the following equation:[15,30]

$$\frac{L_g}{L}\Gamma' g_{th}' = \alpha_{wcore} + \alpha_m \tag{3}$$

$$\alpha_m = \frac{1}{L}\ln\frac{1}{R} \tag{4}$$

Where Γ' is the confinement factor, g_{th}' is the threshold gain, L is the length of the core−shell rod, L_g is the length where gain occurs (equals to the excitation spot size), α_{wcore} is the waveguide loss for GaN core, and R is reflectivity of the two end faces. R is related to the refractive index difference between GaN and air.[38] As R for 372 nm is about 0.202 and R for 408 nm is about 0.185,[39,40] α_m for 372 nm is almost the same as α_m for 408 nm, and α_{wcore} for 372 nm is bigger than that for 408 nm.[40,41] Γ' for 372 nm is smaller than Γ' for 408 nm, as the high order modes tend to shift their field distribution toward the side facets with increasing wavelength. Based on the above analysis, in conjunction with eqs 3 and 4, we can obtain that the g_{th}' for 372 nm will be higher than the g_{th}' for 408 nm. More importantly, when excited by a Nd:YAG laser (355 nm), the InGaN shell with high In composition has a bigger absorption

DOI: 10.1021/acsnano.7b01417
ACS Nano XXXX, XXX, XXX−XXX

coefficient than that with low In composition.[20,21] Under the same excitation power density, the InGaN shell with low In composition is more difficult to achieve a threshold gain. This also makes the g_{th}' for 372 nm higher than the g_{th}' for 408 nm, which is consistent with the experimental results (Figure 5b). Due to the existence of the decoupling effect, Γ' is much smaller than Γ_0. This is why g_{th}' for the core−shell rod is larger than g_{th}^0 for GaN core. When the length of the GaN core and the growth condition of InGaN shell are changed, we may get a WCVL with a higher variation rate. Further investigation is still in progress. This idea of WCVL structural design can be applied in many material systems and is not limited to the III−V nitrides.

CONCLUSIONS

In summary, a core−shell structure that decouples the gain medium and optical cavity is presented, and the corresponding mechanism for wavelength modulation is explained. Based on the above structure, one kind of WCVL is demonstrated on a single GaN/InGaN core−shell microrod without modifying the geometry of resonant cavity or cutting the microrod. Using this method, we can control lasing wavelength flexibly and repeatedly on a single facilely synthesized microrod and realize very high wavelength variation rates (3.6 nm/μm). Furthermore, we determine the lasing oscillation mode of our core−shell WCVL and qualitatively analyze the threshold of different excitation points (different lasing wavelengths). By analyzing α_m, α_{wcore}, and Γ' for different wavelengths, we can obtain that the g_{th}' for 372 nm is higher than the g_{th}' for 408 nm. More importantly, under the same excitation power density, the InGaN shell with low In composition is more difficult to achieve a threshold gain. This also makes the g_{th}' for 372 nm higher than the g_{th}' for 408 nm, which is consistent with the experimental results. This idea of WCVL structural design can be applied in many material systems, which demonstrates a big application potential in numerous fields.

METHODS

Sample Preparation. The GaN/InGaN core−shell structure in this study is synthesized on sapphire substrates by a Thomas Swan CCS-MOCVD system. First, to obtain high crystalline quality GaN microrods, the substrate is loaded into showerhead MOCVD equipment for GaN microrods growth. Before growth, the substrate is heated to 1100 °C for 20 min under an atmosphere of ammonia. Then GaN microrods are grown at 1040 °C under a pressure of 200 Torr. Trimethylgallium (TMGa) and ammonia (NH_3) are used as the precursors in the growth. The TMGa flow rate is maintained at 30 sccm, and the NH_3 flow rate is kept at 240 sccm. Pure hydrogen (H_2) is used as the carrier gas. Then InGaN shell is radially grown on the GaN core at 750 °C for 300 s. Trimethylgallium (TMGa), trimethylindium (TMIn), and ammonia (NH_3) are used as the precursors in the growth. The TMGa and TMIn flow rate is maintained at 2.2 and 225 sccm. The NH_3 flow rate is 8000 sccm. Pure nitrogen (N_2) is used as the carrier gas.

Experiment. The room-temperature microphotoluminescence spectrum is inspected under the excitation of a 325 nm continuous wave He−Cd laser. The lasing characteristics of the GaN and core−shell microrods are investigated using confocal microphotoluminescence spectroscopy at room temperature. The third harmonic (355 nm) of a Nd:YAG laser (1 kHz, 1 ns pulse width) is used as the excitation source. The type of the spectrometer is an Andor/SR-500i-D1-R, with a resolution of 0.08 nm. The microstructure of the GaN/InGaN core−shell rods is observed by SEM (FEI NANOSEM 430) and TEM (FEI TECNAI F30).

ASSOCIATED CONTENT

Supporting Information

The Supporting Information is available free of charge on the ACS Publications website at DOI: 10.1021/acsnano.7b01417.

Figures S1−S2 showing the PL spectrum of a GaN/InGaN core−shell rod and the 2D optical field distributions of different modes supported by the core−shell structure (PDF)

AUTHOR INFORMATION

Corresponding Authors

*E-mail: huxd@pku.edu.cn.

*E-mail: cfpan@binn.cas.cn.

ORCID

Caofeng Pan: 0000-0001-7693-5388

Xiaodong Hu: 0000-0002-1319-1630

Notes

The authors declare no competing financial interest.

ACKNOWLEDGMENTS

The authors thank the support from National Natural Science Foundation of China (nos. 61334005, 61225019, 61521004, 61376060, 61405040, and 61675027), National Basic Research Program of China (nos. 2012CB619300, 2013CB632800, and 2016YFA0202703), National Key R&D Program of China (no. 2016YFB0401801), and Science Challenge Project (no. JCKY2016212A503). The authors also thank all the staff during the measurements at the beamline 1W1A at BSRF.

REFERENCES

(1) Yan, R.; Gargas, D.; Yang, P. Nanowire Photonics. *Nat. Photonics* **2009**, *3*, 569−576.

(2) Hansch, T. W.; Shahin, I. S.; Schawlow, A. L. High-Resolution Saturation Spectroscopy of the Sodium D Lines with a Pulsed Tunable Dye Laser. *Phys. Rev. Lett.* **1971**, *27*, 707.

(3) Pascu, M. L.; Moise, N.; Staicu, A. Tunable Dye Laser Applications in Environment Pollution Monitoring. *J. Mol. Struct.* **2001**, *598*, 57−64.

(4) Buus, J.; Murphy, E. J. Tunable Lasers in Optical Networks. *J. Lightwave Technol.* **2006**, *24*, 5−11.

(5) Pan, A.; Yang, H.; Liu, R.; Yu, R.; Zou, B.; Wang, Z. L. Color-Tunable Photoluminescence of Alloyed $CdS_{(x)}Se_{(1-x)}$ Nanobelts. *J. Am. Chem. Soc.* **2005**, *127*, 15692−15693.

(6) Liu, Y.; Zapien, J. A.; Shan, Y. Y.; Geng, C. Y.; Lee, C. S.; Lee, S. T. Wavelength-Controlled Lasing in $Zn_xCd_{1-x}S$ Single-Crystal Nanoribbons. *Adv. Mater.* **2005**, *17*, 1372−1377.

(7) Pan, A.; Liu, R.; Wang, F.; Xie, S.; Zou, B.; Zacharias, M.; Wang, Z. L. High-Quality Alloyed CdS_xSe_{1-x} Whiskers as Waveguides with Tunable Stimulated Emission. *J. Phys. Chem. B* **2006**, *110*, 22313−22317.

(8) Liu, Y. K.; Zapien, J. A.; Shan, Y. Y.; Tang, H.; Lee, C. S.; Lee, S. T. Wavelength-Tunable Lasing in Single-Crystal $CdS_{1-X}Se_X$ Nanoribbons. *Nanotechnology* **2007**, *18*, 365606.

(9) Pan, A.; Zhou, W.; Leong, E. S.; Liu, R.; Chin, A. H.; Zou, B. S.; Ning, C. Z. Continuous Alloy-Composition Spatial Grading and Superbroad Wavelength-Tunable Nanowire Lasers on A Single Chip. *Nano Lett.* **2009**, *9*, 784−788.

(10) Song, J. J.; Wang, W. C. Laser Oscillations in the Bound-Excitonic Region of CdS. *J. Appl. Phys.* **1984**, *55*, 660−664.

(11) Antoine-Vincent, N.; Natali, F.; Mihailovic, M.; Vasson, A.; Leymaire, J.; Disseix, P.; Byrne, D.; Semond, F.; Massies, J. Determination of the Refractive Indices of AlN, GaN, and $Al_xGa_{1-x}N$ Grown on (111) Si Substrates. *J. Appl. Phys.* **2003**, *93*, 5222.

DOI: 10.1021/acsnano.7b01417
ACS Nano XXXX, XXX, XXX−XXX

(12) Xu, J. Y.; Zhuang, X. J.; Guo, P. F.; Huang, W. Q.; Hu, W.; Zhang, Q. L.; Wan, Q.; Zhu, X. L.; Yang, Z. Y.; Tong, L. M.; Duan, X. F.; Pan, A. L. Asymmetric Light Propagation in Composition-Graded Semiconductor Nanowires. *Sci. Rep.* **2012**, *2*, 820.
(13) Yang, Z. Y.; Wang, D. L.; Meng, C.; Wu, Z. M.; Wang, Y.; Ma, Y. G.; Dai, L.; Liu, X. W.; Hasan, T. F.; Liu, X.; Yang, Q. Broadly Defining Lasing Wavelengths in Single Bandgap-Graded Semiconductor Nanowires. *Nano Lett.* **2014**, *14*, 3153−3159.
(14) Lu, Y.; Gu, F.; Meng, C.; Yu, H.; Ma, Y.; Fang, W.; Tong, L. Multicolour Laser From A Single Bandgap-Graded CdSSe Alloy Nanoribbon. *Opt. Express* **2013**, *21*, 22314−22319.
(15) Li, J.; Meng, C.; Liu, Y.; Wu, X.; Lu, Y.; Ye, Y.; Dai, L.; Tong, L.; Liu, X.; Yang, Q. Wavelength Tunable CdSe Nanowire Lasers Based on the Absorption -Emission-Absorption Process. *Adv. Mater.* **2013**, *25*, 833−837.
(16) Liu, X. F.; Zhang, Q.; Xiong, Q. H.; Sum, T. C. Tailoring the Lasing Modes in Semiconductor Nanowire Cavities Using Intrinsic Self-Absorption. *Nano Lett.* **2013**, *13*, 1080−1085.
(17) Liu, X. F.; Zhang, Q.; Yip, J. N.; Xiong, Q. H.; Sum, T. C. Wavelength Tunable Single Nanowire Lasers Based on Surface Plasmon Polariton Enhanced Burstein-Moss Effect. *Nano Lett.* **2013**, *13*, 5336−5343.
(18) Pauzauskie, P. J.; Sirbuly, D. J.; Yang, P. D. Semiconductor Nanowire Ring Resonator Laser. *Phys. Rev. Lett.* **2006**, *96*, 143903.
(19) Xiao, Y.; Meng, C.; Wu, X. Q.; Tong, L. M. Single Mode Lasing in Coupled Nanowires. *Appl. Phys. Lett.* **2011**, *99*, 023109.
(20) Schenk, H. P. D.; Leroux, M.; de Mierry, P. Luminescence and Absorption in InGaN Epitaxial Layers and the Van Roosbroeck-Shockley Relation. *J. Appl. Phys.* **2000**, *88*, 1525−1534.
(21) Siozade, L.; Leymarie, J.; Disseix, P.; Vasson, A.; Mihailovic, M.; Grandjean, N.; Leroux, M.; Massies, J. Modelling of Thermally Detected Optical Absorption and Luminescence of (In,Ga)N/GaN Heterostructures. *Solid State Commun.* **2000**, *115*, 575−579.
(22) Dobrovolsky, A.; Stehr, J. E.; Sukrittanon, S.; Kuang, Y. J.; Tu, C. W.; Chen, W. M.; Buyanova, I. A. Fabry-Perot Microcavity Modes in Single GaP/GaNP Core/Shell Nanowires. *Small* **2015**, *11*, 6331−6337.
(23) Yan, X.; Zhang, X.; Li, J. H.; Wu, Y.; Cui, J. G.; Ren, X. M. Fabrication and Optical Properties of GaAs/InGaAs/GaAs Nanowire Core−Multishell Quantum Well Heterostructures. *Nanoscale* **2015**, *7*, 1110−1115.
(24) Qian, F.; Li, Y.; Gradecak, S.; Park, H. G.; Dong, Y. J.; Ding, Y.; Wang, Z. L.; Lieber, C. M. Multi-Quantum-Well Nanowire Heterostructures for Wavelength-Controlled Lasers. *Nat. Mater.* **2008**, *7*, 701−706.
(25) Leung, M. M. Y.; Djurišić, A. B.; Li, E. H. Refractive Index of InGaN/GaN Quantum Well. *J. Appl. Phys.* **1998**, *84*, 6312−6317.
(26) Maslov, A. V.; Ning, C. Z. Reflection of Guided Modes in A Semiconductor Nanowire Laser. *Appl. Phys. Lett.* **2003**, *83*, 1237−1239.
(27) Röder, R.; Ploss, D.; Kriesch, A.; Buschlinge, R.; Geburt, S.; Peschel, U.; Ronning, C. Polarization Features of Optically Pumped CdS Nanowire Lasers. *J. Phys. D: Appl. Phys.* **2014**, *47*, 394012.
(28) Saxena, D.; Mokkapati, S.; Parkinson, P.; Jiang, N.; Gao, Q.; Tan, H. H.; Jagadish, C. Optically Pumped Room-Temperature GaAs Nanowire Lasers. *Nat. Photonics* **2013**, *7*, 963−968.
(29) Röder, R.; Sidiropoulos, T. P. H.; Buschlinger, R.; Riediger, M.; Peschel, U.; Oulton, R. F.; Ronning, C. Mode Switching and Filtering in Nanowire Lasers. *Nano Lett.* **2016**, *16*, 2878−2884.
(30) Arafin, S.; Liu, X. H.; Mi, Z. T. Review of Recent Progress of III-Nitride Nanowire Lasers. *J. Nanophotonics* **2013**, *7*, 074599.
(31) Gradecak, S.; Qian, F.; Li, Y.; Park, H. G.; Lieber, C. M. GaN Nanowire Lasers with Low Lasing Thresholds. *Appl. Phys. Lett.* **2005**, *87*, 173111.
(32) Amari, H.; Ross, I. M.; Wang, T.; Walther, T. Characterization of InGaN/GaN Epitaxial Layers by Aberration Corrected TEM/STEM. *Phys. Status Solidi (C)* **2012**, *9*, 546−549.
(33) Tsuchiya, T.; Shimizu, J.; Shirai, M.; Aoki, M. InGaAlAs Selective-Area Growth on an InP Substrate by Metalorganic Vapor-Phase Epitaxy. *J. Cryst. Growth* **2005**, *276*, 439−445.
(34) Feng, W.; Kuryatkov, V. V.; Chandolu, A.; Song, D. Y.; Pandikunta, M.; Nikishin, S. A.; Holtz, M. Green Light Emission From InGaN Multiple Quantum Wells Grown on GaN Pyramidal Stripes Using Selective Area Epitaxy. *J. Appl. Phys.* **2008**, *104*, 103530.
(35) Zimmler, M. A.; Bao, J. M.; Capasso, F.; Muller, S.; Ronning, G. Laser Action in Nanowires: Observation of the Transition From Amplified Spontaneous Emission to Laser Oscillation. *Appl. Phys. Lett.* **2008**, *93*, 051101.
(36) Baek, H.; Hyun, J. K.; Chung, K.; Oh, H.; Yi, G. C. Selective Excitation of Fabry-Perot or Whispering-Gallery Mode-Type Lasing in GaN Microrods. *Appl. Phys. Lett.* **2014**, *105*, 201108.
(37) Wiersig, J. Hexagonal Dielectric Resonators and Microcrystal Lasers. *Phys. Rev. A: At., Mol., Opt. Phys.* **2003**, *67*, 023807.
(38) Kawashima, T.; Yoshikawa, H.; Adachi, S. Optical Properties of Hexagonal GaN. *J. Appl. Phys.* **1997**, *82*, 3528−3535.
(39) Yu, G.; Wang, G.; Ishikawa, H.; Umeno, M.; Soga, T.; Egawa, T.; Watanabe, J.; Jimbo, T. Optical Properties of Wurtzite Structure GaN on Sapphire Around Fundamental Absorption Edge (0.78−4.77 eV) by Spectroscopic Ellipsometry and the Optical Transmission Method. *Appl. Phys. Lett.* **1997**, *70*, 3209−3211.
(40) Muth, J. F.; Lee, J. H.; Shmagin, I. K.; Kolbas, R. M., Jr; Casey, H. C.; Keller, B. P.; Mishra, U. K.; DenBaars, S. P. Absorption Coefficient, Energy Gap, Exciton Binding Energy, and Recombination Lifetime of GaN Obtained From Transmission Measurements. *Appl. Phys. Lett.* **1997**, *71*, 2572−2574.
(41) Zimmler, M. A.; Capasso, F.; Müller, S.; Ronning, C. Optically Pumped Nanowire Lasers: Invited Review. *Semicond. Sci. Technol.* **2010**, *25*, 024001.

DOI: 10.1021/acsnano.7b01417
ACS Nano XXXX, XXX, XXX−XXX